Measurement Science
and Technology

PAPER

Stochastic modeling of between-receiver single-differenced ionospheric delays and its application to medium baseline RTK positioning

To cite this article: Xiaolong Mi *et al* 2019 *Meas. Sci. Technol.* **30** 095008

IOP Publishing Measurement Science and Technology
Meas. Sci. Technol. **30** (2019) 095008 (10pp) https://doi.org/10.1088/1361-6501/ab11b5

Stochastic modeling of between-receiver single-differenced ionospheric delays and its application to medium baseline RTK positioning

Xiaolong Mi[1,2], Baocheng Zhang[1] and Yunbin Yuan[1]

[1] State Key Laboratory of Geodesy and Earth's Dynamics, Institute of Geodesy and Geophysics, Wuhan, People's Republic of China
[2] University of Chinese Academy of Sciences, Beijing, People's Republic of China

E-mail: b.zhang@whigg.ac.cn

Received 21 January 2019, revised 13 March 2019
Accepted for publication 20 March 2019
Published 29 July 2019

Abstract

Global navigation satellite system (GNSS) carrier phase integer ambiguity resolution is one of the key issues and challenges for precise relative positioning. For baselines greater than 10 km, integer ambiguity resolution becomes difficult because the ionospheric delay effects on the single-differenced (SD) observations are significant. One way to deal with this difficulty is to weight the ionospheric delays, instead of treating them in a deterministic way, giving rise to the so-called ionosphere-weighted model. With this model relative positioning technology is enabled to work with much larger inter-station distances than its current status. Here we seek to gain insight into how to reasonably weight the SD ionospheric delays, normally introduced in the ionosphere-weighted model as pseudo observables, which consists of two sequential steps. The first step seeks to construct realistic stochastic models for the GNSS observables with the ionosphere-fixed model where the SD ionospheric delays are assumed to be absent. With the results so obtained in the second step we estimate the variance of the SD ionospheric delays with the ionosphere-float model, in which the SD ionospheric delays are assumed to be fully unknown. Numerical tests based on GPS data from the National Geodetic Survey CORS network demonstrate a clear improvement in medium baseline real time kinematic (RTK) positioning performance, as compared to the ionosphere-weighted model that employs the unrealistic stochastic models for the pseudo SD ionospheric observables.

Keywords: GNSS, ionosphere-weighted model, between-receiver single-differenced, medium baseline, RTK

(Some figures may appear in colour only in the online journal)

Introduction

Successful carrier phase integer ambiguity resolution is crucial to precise relative global navigation satellite system (GNSS) positioning (Teunissen 1997, Odijk 2000a, Li *et al* 2010). For short baselines of a few km, it is easy to resolve the ambiguities into integers as the ionosphere-fixed model applies in this case (Teunissen 1998, Odijk 2000b, Odolinski *et al* 2015a). As the baseline length increases, resolution of the ambiguities can be a challenging task, since the ionospheric effects on the GNSS observations become so significant that the ionosphere-float model may apply (Julien *et al* 2004, Wielgosz 2011).

Since the ionospheric delay is one of the predominant errors in precise relative positioning, several techniques have been developed to deal with its influence (Odijk 2002, Wanninger 2002, Euler 2004, Grejner-Brzezinska *et al* 2004). One typical way is to take advantage of the ionosphere-weighted model in case of medium baseline, in which the SD ionospheric delays

are treated stochastically instead of deterministically (Odijk 2000c, Liu 2001, Wielgosz 2005, Zhou and Wang 2013). The key of the ionosphere-weighted model lies in stochastic modelling of the between-receiver single-differenced (SD) ionospheric delays that are introduced as pseudo observables; this observable, added to the original GNSS observation equations, are however often improperly weighted, which can degrade the performance of the ionosphere-weighted model (Wang *et al* 2016).

In the medium baseline case, it is reasonable to assume the value of the (pseudo) SD ionospheric observables to be zero. The key task is then how to weight this observable reasonably, which, in this contribution, is accomplished in two sequential steps. In the first step, the ionosphere-fixed model is derived based on the SD GNSS observation equations with baseline components and integer ambiguities correctly fixed, so as to construct the stochastic model for the GNSS observables. This procedure is also known as the variance component estimation (VCE) technique (Tiberius *et al* 2000, Wang *et al* 2002, Tiberius and Kenselaar 2003, Amiri-Simkooei 2013). The second step concerns the application of the ionosphere-float model, using the results of the first step, to empirically determine the variances of the SD ionospheric delays. Experimental verification is subsequently carried out.

Method

This section begins with a review of the ionosphere-float, -fixed and -weighted models, focusing on how to address them with the rank deficiencies underlying the GNSS observation equations. Next, we briefly introduce how to use the VCE technology to obtain correct stochastic models of the GNSS observables. We close this section with a description on how to perform stochastic modeling of the SD ionosphere observables.

Models

Consider receivers r, u tracking a GNSS system $s_* = 1_*, ..., m_*$ on frequencies $j_* = 1_*, \ldots, f_*$, where s_* and m_* are the number of satellites and frequencies of the system, respectively. Note that the baseline length of our study was not greater than 100 km, so the tropospheric delay has not been treated as one type of unknown parameters; instead, we assume that the Saastamoinen troposphere model can effectively eliminate its impact (Saastamoinen 1972, Goad 1974, Böhm *et al* 2007).

Ionosphere-float model. In this case, the ionospheric effects on the GNSS data are so significant that they should be treated as fully unknown parameters. Receiver code and phase delays left after single-differencing are responsible for the rank deficiencies underlying the observation equations. We can obtain full-rank equations by using the *S*-system theory (Teunissen *et al* 2010). Table 1 summarizes the number of rank deficiencies and the *S*-basis choice of the ionosphere-float, -fixed and -weighted models.

Table 1. The number of rank deficiencies and the S-basis choice of the ionosphere-float, ionosphere-fixed and ionosphere-weighted models, where f_* stands for the number of frequencies.

Model	Rank defects	S-basis choice
Ionosphere-float	$2+f_*$	$\Delta d_{ru,1_*}, \Delta d_{ru,2_*}, \Delta N^{1_*}_{ru,j_*}$
Ionosphere-fixed	$1+f_*$	$\Delta d_{ru,1_*}, \Delta N^{1_*}_{ru,j_*}$
Ionosphere-weighted	$1+f_*$	$\Delta d_{ru,1_*}, \Delta N^{1_*}_{ru,j_*}$

The rank deficiencies for the ionosphere-float model comes from three aspects, which are the rank deficiencies between the receiver clock and code/phase delays, those between the clocks, code/phase delays and ionosphere, and those between the phase delays and ambiguities. After choosing some of the parameters as the S-basic choice, as suggested in table 1, the SD full-rank observation equations read

$$\begin{aligned}\Delta\rho^{s_*}_{ru,j_*} &= c_u^{s_*T}\Delta x_{ru} + \Delta\tilde{dt}_{ru} + \Delta\tilde{d}_{ru,j_*} + \mu_{j_*}\Delta\tilde{I}^{s_*}_{ru}\\ \Delta\phi^{s_*}_{ru,j_*} &= c_u^{s_*T}\Delta x_{ru} + \Delta\tilde{dt}_{ru} + \Delta\tilde{\delta}_{ru,j_*} - \mu_{j_*}\Delta\tilde{I}^{s_*}_{ru} + \lambda_{j_*}\nabla\Delta\tilde{N}^{1s_*}_{ru}\end{aligned} \quad (1)$$

where $\Delta(.)_{ru} = (.)_u - (.)_r$ is the notation for SD, the SD code and phase are denoted as $\Delta\rho^{s_*}_{ru,j_*}, \Delta\phi^{s_*}_{ru,j_*}$, respectively, $c_u^{s_*T}$ is the line-of-sight unit vector from receiver u to the satellites obtained from linearizing the system of equations with respect to the receiver coordinates, which can be expressed as $c_u^{s_*T} = (x^s - x_u)^T / \|x^s - x_u\|$ and $\mu_{j_*} = f^2_{1_*}/f^2_{j_*}$ is the conversion of ionospheric delay from frequency 1_* to j_* among a GNSS, while λ_{j_*} denotes the wavelength for frequency j_*. Table 2 presents the unknown parameters and their interpretations in equation (1).

Ionosphere-fixed model. Ionosphere delays can be eliminated sufficiently in single differencing for a short baseline of a few km, which increases the redundancy and thus strengthens the model. However, even in this situation, the observation equations are not of full-rank (Odolinski *et al* 2013). Notably in table 1, $\Delta d_{ru,2_*}$is no longer selected as a S-basis choice compared to the ionosphere-float model because the rank defects between the receiver clocks, code/phase delays and ionosphere are eliminated.

After the rank deficiencies have been solved, the ionosphere-fixed full-rank observation equations are as follows:

$$\begin{aligned}\Delta\rho^{s_*}_{ru,j_*} &= c_u^{s_*T}\Delta x_{ru} + \Delta\tilde{\tilde{dt}}_{ru} + \Delta\tilde{\tilde{d}}_{ru,j_*}\\ \Delta\phi^{s_*}_{ru,j_*} &= c_u^{s_*T}\Delta x_{ru} + \Delta\tilde{\tilde{dt}}_{ru} + \Delta\tilde{\tilde{\delta}}_{ru,j_*} + \lambda_{j_*}\nabla\Delta\tilde{N}^{1s_*}_{ru}.\end{aligned} \quad (2)$$

Similar to tables 2 and 3, this interprets the unknown parameters.

Ionosphere-weighted model. For this model the *S*-basis choice is the same as the ionosphere-fixed model, so we can obtain an ionosphere-weighted model of full rank easily as follows:

$$\begin{aligned}\Delta\rho^{s_*}_{ru,j_*} &= c_u^{s_*T}\Delta x_{ru} + \Delta\tilde{\tilde{dt}}_{ru} + \Delta\tilde{\tilde{d}}_{ru,j_*} + \mu_{j_*}\Delta I^{s_*}_{ru}\\ \Delta\phi^{s_*}_{ru,j_*} &= c_u^{s_*T}\Delta x_{ru} + \Delta\tilde{\tilde{dt}}_{ru} + \Delta\tilde{\tilde{\delta}}_{ru,j_*} - \mu_{j_*}\Delta I^{s_*}_{ru} + \lambda_{j_*}\nabla\Delta\tilde{N}^{1s_*}_{ru}\\ \Delta\hat{I}^{s_*}_{ru} &= \Delta I^{s_*}_{ru}\end{aligned} \quad (3)$$

Table 2. Estimable unknown parameters and their interpretations in the ionosphere-float model, where s_* and j_* are the number of satellites and frequencies of one GNSS.$\mu_{j_*} = f_{1_*}^2/f_{j_*}^2$ is the frequency-dependent factor that is used to convert ionospheric delay from the first frequency to other frequencies of one system.

Notation and interpretation	Estimable parameter
$\Delta x_{ru} = \Delta x_u - \Delta x_r$	Relative receiver coordinates
$\Delta\tilde{dt}_{ru} = \Delta dt_{ru} + \frac{\mu_{2_*}}{\mu_{2_*}-\mu_{1_*}}\Delta dt_{ru,1_*} - \frac{\mu_{1_*}}{\mu_{2_*}-\mu_{1_*}}\Delta dt_{ru,2_*}$	Relative receiver clock with code delays on $j_* = 1_*, 2_*$
$\Delta\tilde{d}_{ru,j_*} = \Delta d_{ru,j_*} - \frac{\mu_{2_*}-\mu_{j_*}}{\mu_{2_*}-\mu_{1_*}}\Delta d_{ru,1_*} + \frac{\mu_{1_*}-\mu_{j_*}}{\mu_{2_*}-\mu_{1_*}}\Delta d_{ru,2_*}$	Relative receiver code delays, where $j_* \geqslant 3$
$\Delta\tilde{\delta}_{ru,j_*} = \Delta\delta_{ru,j_*} - \frac{\mu_{2_*}+\mu_{j_*}}{\mu_{2_*}-\mu_{1_*}}\Delta d_{ru,1_*} + \frac{\mu_{1_*}+\mu_{j_*}}{\mu_{2_*}-\mu_{1_*}}\Delta d_{ru,2_*} + \lambda_{j_*}\Delta N_{ru,j_*}^{1_*}$	Relative receiver phase delays, where $j_* \geqslant 1$
$\Delta\tilde{I}_{ru}^{s_*} = \Delta I_{ru}^{s_*} + \frac{\Delta d_{ru,2_*}-\Delta d_{ru,1_*}}{\mu_{2_*}-\mu_{1_*}}$	Relative ionospheric delays biased by between-receiver differential code biases (BR-DCB), where $s_* \geqslant 1$
$\nabla\Delta\tilde{N}_{ru}^{1s_*} = \Delta N_{ru}^{s_*} - \Delta N_{ru}^{1_*}$	DD integer ambiguities, where $j_* \geqslant 1, s_* \geqslant 2$

where $\Delta\widehat{I}_{ru}^{s_*}$ denotes the additional ionosphere observables. The estimable unknowns here have the same interpretation as those in the ionosphere-fixed model (see table 3).

Interestingly, ionosphere-fixed and ionosphere-float models are two special cases of the ionosphere-weighted model. When $\sigma_I = 0$ (or 'infinite' weight), the ionospheric delays are, strictly speaking, not stochastic variables, but deterministic quantities, implying that they are completely known beforehand. In this case the ionosphere-weighted model reduces to the so-called ionosphere-fixed model. On the other hand, when $\sigma_I = \infty$ (or 'zero' weight), the ionospheric observations do not contribute at all to the solution of the model, they are assumed to be completely unknown parameters, and the solution equals that of the ionosphere-float model.

Variance component estimation (VCE)

The functional model depicts the relations between measured and unknown parameters (Zhang *et al* 2018); meanwhile, the stochastic model shows the accuracy (variance) and correlation (covariance) of observations (Grodecki 2001). The optimal parameter estimation, which guarantees precise positioning in GNSS applications, can only be addressed by accurate stochastic models (Crocetto *et al* 2000, Liu *et al* 2004, Teunissen and Amiri-Simkooei 2008). Therefore, different observations should be weighted reasonably so as to adequately reach the best linear unbiased estimators (BLUE). This can be achieved by employing the VCE methods with which the contribution of different noise components to the stochastic model can be estimated.

The VCE methods have been widely applied to the standard least squares (SLS) problem in which only the observation vector is subject to heterogeneous noise. Several VCE methods exist, such as minimum norm quadratic unbiased estimation (MINQUE) and the Helmert method (Amiri-Simkooei 2007, Xu *et al* 2006). We use least-squares VCE (LS-VCE) because it is widely used in GNSS (Ananga *et al* 1994, Li *et al* 2008, Amiri-Simkooei and Jazaeri 2012).

In VCE for GNSS measurements, the SD model is favored for several reasons. First, the mathematical correlation is not introduced, leading to the variance matrix being a diagonal matrix. Then, it is very convenient to evaluate stochastic characteristics based on SD residuals. Furthermore, zero-short baselines are also favored because the ambiguity can be fixed easily and the effects of residual tropospheric, ionospheric and multipath errors can be neglected.

Table 3. Unknown parameters and their interpretation for ionosphere-fixed and ionosphere-weighted models, where s_* and j_* are the number of satellites and frequencies of one GNSS.

Notation and interpretation	Estimable parameter
$\Delta x_{ru} = \Delta x_u - \Delta x_r$	Relative receiver coordinates
$\Delta\tilde{\tilde{dt}}_{ru} = \Delta dt_{ru} + \Delta dt_{ru,1_*}$	Relative receiver clock with code delays on $j_* = 1$
$\Delta\tilde{\tilde{d}}_{ru,j_*} = \Delta d_{ru,j_*} - \Delta d_{ru,1_*}$	Relative BR-DCB, where $j_* \geqslant 2_*$
$\Delta\tilde{\tilde{\delta}}_{ru,j_*} = \Delta\delta_{ru,j_*} - \Delta d_{ru,1_*} + \lambda_{j_*}\Delta N_{ru,j_*}^{1_*}$	Relative receiver phase delays, where $j_* \geqslant 1_*$
$\Delta I_{ru}^{s_*}$	Relative ionospheric delays
$\nabla\Delta\tilde{N}_{ru}^{1s_*} = \Delta N_{ru}^{s_*} - \Delta N_{ru}^{1_*}$	DD integer ambiguities, where $j_* \geqslant 1_*, s_* \geqslant 2$

The ionosphere-fixed model with *a priori* known baseline components and integer ambiguities is widely adopted. The rank deficiencies of the ionosphere-fixed model has been solved; thus we can easily obtain the equation used in VCE, which read

$$\begin{aligned}\Delta\tilde{\rho}_{ru,j_*}^{s_*} &= \Delta\rho_{ru,j_*}^{s_*} - c_u^{s_*T}\Delta x_{ru} = \Delta\bar{\bar{d}}_{ru,j_*}\\ \Delta\tilde{\phi}_{ru,j_*}^{s_*} &= \Delta\phi_{ru,j_*}^{s_*} - c_u^{s_*T}\Delta x_{ru} - \lambda_{j_*}\nabla\Delta\tilde{N}_{ru}^{1s_*} = \Delta\bar{\bar{\delta}}_{ru,j_*}\end{aligned} \quad (4)$$

where $\Delta\bar{\bar{d}}_{ru,j_*} = \Delta dt_{ru} + \Delta d_{ru,j_*}$ and $\Delta\bar{\bar{\delta}}_{ru,j_*} = \Delta dt_{ru} + \Delta\delta_{ru,j_*}$. In this study, for each type of observation, only one unknown parameter is presented. Assuming m satellites are tracked at the same time, only one system is used for the ease of presentation, and the SD equation of one observable type reads

$$\Delta y = e_m\Delta x \quad (5)$$

where Δy denotes $\Delta\tilde{\rho}_{ru,j_*}^{s_*}$, $\Delta\tilde{\delta}_{ru,j_*}^{s_*}$,$e_m$ expresses m vectors filled with ones and Δx represents only one unknown in a class of observational equations ($\Delta\bar{\bar{d}}_{ru,j_*}$, $\Delta\bar{\bar{\delta}}_{ru,j_*}$). The VCE formulas derived in this study are based on the least-squares residuals $V_i = \Delta y - e_m\Delta\tilde{x}$, in which i denotes different types of measurements and $\Delta\tilde{x}$ represents the least squares estimate

Table 4. An overview of GPS data sets used in VCE.

Station name	Receiver type	Antenna type	Location	Observation period
CUT0	TRIMBLE NETR9	TRM59800.00	115.89 °E, 32.00 °S	2018, day 220
CUAI	SEPT POLARXS	TRM59800.00		
CUTA	TRIMBLE NETR9	TRM59800.00		

of the parameter. The formula for estimating the (co)variances is

$$\delta_{ru,ij} = \delta_{r,ij} + \delta_{u,ij} = \frac{V_i^T V_j}{m-1} \tag{6}$$

which makes the VC matrix of the SD observable.

With two receivers r and u, if they are of the same type, the (co)variances of the undifferenced observations can be obtained by $\delta_{r,ij} = \delta_{u,ij} = \frac{\delta_{ru,ij}}{\sqrt{2}}$. After the (co)variances of undifferenced observations are solved, we can calculate the cross correlation (ρ_{ij}) between observations of different types as follows:

$$\rho_{ij} = \frac{\delta_{ij}}{\sqrt{\delta_i}\sqrt{\delta_j}} \tag{7}$$

where δ_{ij} represents covariance, δ_i and δ_j denotes variance of different types. With the above formula, we can readily formulate the stochastic model for each of the receivers used.

Weighting the SD ionospheric observables

The SD ionospheric delays of one satellite in five minutes can be adequately assumed to be constant, because of the very small variation of elevation angle over this short period. Thus, we intend to use the ionosphere-float model to separate the SD ionospheric delay of each satellite and calculate the STD of the SD ionospheric delays as the variance. For the accurate acquisition of SD ionospheric delays, the ionosphere-float model with *a priori* known baseline components and integer ambiguities is adopted, which reads

$$\begin{aligned}\Delta\overline{\overline{\rho}}^{s*}_{ru,j*} &= \Delta\widetilde{\rho}^{s*}_{ru,j*} - c^{s*T}_{u,j*}\Delta x_{ru} = \Delta\tilde{d}t_{ru,j*} + \mu_{j*}\Delta\widetilde{I}^{s*}_{ru} \\ \Delta\overline{\overline{\phi}}^{s*}_{ru,j*} &= \Delta\widetilde{\phi}^{s*}_{ru,j*} - c^{s*T}_{u,j*}\Delta x_{ru} - \lambda_{j*}\Delta\widetilde{N}^{1s*}_{ru,j*} \\ &= \Delta\tilde{d}t_{ru,j*} + \Delta\tilde{\delta}_{ru,j*} + \mu_{j*}\Delta\widetilde{I}^{s*}_{ru}\end{aligned} \tag{8}$$

where the parameters have the same interpretation as the ionosphere-float model. Note, importantly, that not only the SD ionospheric delays but also the BR-DCBs are contained in $\Delta\widetilde{I}^{s*}_{ru}$, which may affect the randomness of the SD ionospheric delays. For this we turn to the ionosphere-weighted model to estimate BR-DCB and apply them to the SD ionospheric delays obtained from the ionosphere-float model (Zhang and Teunissen 2015, Zhang and Teunissen 2016). For the empirical ionosphere-weighted model adopted, the variance of the SD ionospheric delays is chosen as a function of the baseline length, say, 0.96 mm/km (Schaffrin and Bock 1988, Odolinski *et al* 2015b).

The variance of the SD ionospheric delays (called ionospheric variance here and in the following) varies as a function of the location, time, solar activity, elevation angle, and baseline length. Fortunately, we focus on baselines less than 60 km, and assume the ionospheric observables to be zero, which eases the difficulty of modeling. Therefore, the ionospheric variance is modeled as a function of the baseline length and elevation angle in this study.

Experimental results

We begin this section by briefly describing the VCE results, followed by illustrating the result of stochastic modeling of SD ionospheric observables, from which we make our major findings. Two experiments are carried out. The first experiment seeks to obtain stochastic models of GNSS observables; the second is used to estimate the ionospheric variance.

Stochastic modeling of GNSS observables

It must be emphasized that, in the data processing throughout this article, the detection, identification and adaptation (DIA) procedure is used to eliminate outliers (Teunissen 2018), and the integer ambiguity resolution is conducted using the LAMBDA method (Teunissen 1995, 1999).

Table 4 summarizes the relevant characteristics of the experimental data sets considered in the first experiment, including the station name, receiver and antenna type, approximate location of the receivers and the time period of the observations.

The three receivers, from a network deployed at the main campus of Curtin University in Perth (Australia), create two short baselines. We collected GPS (phase and code) observations at both L1 (1575.42 MHZ) and L2 (1227.60 MHZ) frequencies, on August 8, 2018. The three receivers CUT0/TA/AI were installed in the roof-top plant room of building 402, where CUTA and CUAI share an antenna and CUT0 and CUTA/CUAI form two baselines of 0.08 m.

In all the cases, the sampling interval of the experimental GPS observations is 1 s, and the elevation cut-off is set to be 25°. We empirically set the undifferenced standard deviation of code as 0.3 m and of phase as 3 mm. For the detailed analysis, we selected an observation span of 10 min (600 epochs) each hour and take the average of all the results as the final result.

We focus first on the baseline of CUT0-CUTA, because the two receivers are of the same type, the standard deviations and correlation coefficients of the undifferenced observation can be easily obtained by the error propagation law, using equations (6) and (7). Table 5 shows the VCE results of the Net R9 receiver, given on the diagonal are the standard deviations in terms of the undifferenced code and phase observation, and the correlation coefficients are given as the off-diagonal elements (top).

Table 5. Standard deviation and correlation coefficients of the Net R9 receiver.

Code/ phase	C1	P2	L1	L2
C1	0.288 m	0.09	0.02	0.00
P2		0.235 m	−0.00	−0.01
L1			1.568 mm	0.38
L2				1.652 mm

Table 6. The standard deviation and correlation coefficients for SEPT POLARXS receiver.

Code/ phase	C1	P2	L1	L2
C1	0.393 m	0.05	−0.02	−0.03
P2		0.187 m	−0.21	−0.26
L1			0.96 mm	0.41
L2				1.31 mm

From the table 5, it can be seen that the precision of the estimated standard deviations is higher than the empirical (code 0.3 m; phase 3 mm). Moreover, there is a correlation between the observations at the two frequencies, especially between the L1 and L2.

We next focus on the CUT0-CUAI, in which the two receivers are of different types, the VCE result of Net R9 should be utilized to calculate the variance-covariance of the SEPT POLARXS receiver, and thus determine the undifferenced VCE result of the receiver. Table 6 shows the VCE results of the SEPT POLARXS receiver, the elements have the same meaning as in table 5. For the sake of simplicity, we only analyzed the results of two types of receivers; the results of other types of receivers can be determined by this method.

It is worth noting that, along with the standard deviation and correlation estimates discussed above, the relation between elevation and observation accuracy is also important for the stochastic model. Equation (9) is considered a reasonable stochastic model function, which reads

$$\hat{\sigma} = \sigma_o(e_1 + e_2 \exp(^{-E^{m*}}/_{E_0})) \tag{9}$$

where $\hat{\sigma}$ and σ_0 represent the final observation accuracy and the accuracy calculated by VCE above, E^{m*} is the elevation of the satellite m_*, and e_1, e_2 and E_0 are the model coefficients.

We only present the modeling results of the Net R9 stochastic model here (see figure 1), which will be applied to the calculation to determine the weights of the SD ionosphere.

Stochastic modeling of SD ionospheric observables

A number of nationwide distributed receivers (see figure 2 for their locations) from the National Geodetic Survey (NGS) CORS network are selected in the second experiment. The network is used to analyze ionospheric variance and the performance of the calculated ionosphere-weighted model. GPS L1 and L2 data were collected at a 1-s sampling rate, on September 5, 2018, which is freely available from the NGS FTP server (ftp://geodesy.noaa.gov/cors/). All stations that participated in this study are equipped with Trimble Net R9 receivers.

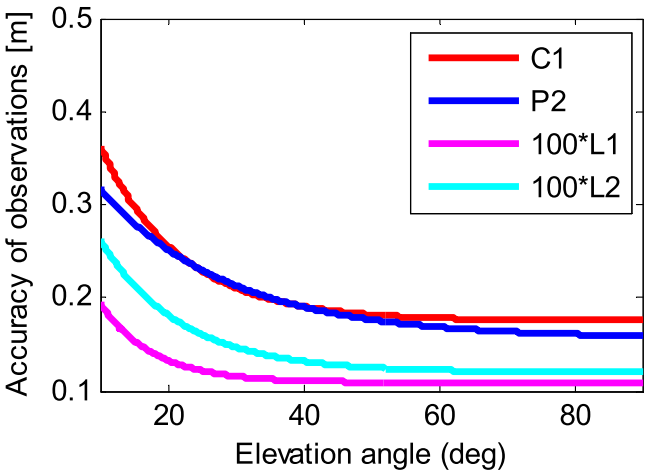

Figure 1. Stochastic model of the Net R9 used in data processing.

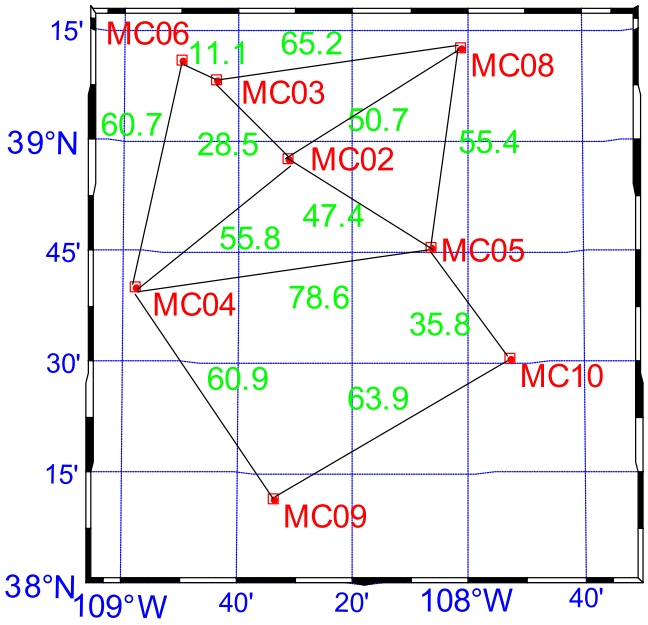

Figure 2. Configuration of the CORS network receivers used in this study (baseline length in kilometers).

In this experiment, we used a cut-off elevation angle of 15° to discard particularly noisy GPS data. These observations were weighted according to the stochastic model results calculated in the first experiment.

Figure 3 depicts 'biased' SD ionospheric delays $\Delta\widetilde{I}^{s*}_{ru}$ (which are biased by BR-DCB, see details in table 2) determined by the ionosphere-float model for the MC02-MC03 baseline from GPS L1 + L2 data collected on September 5, 2018. We split this figure into six panels for clearer presentation, with each panel showing the result of one satellite. Moreover, the red line in each panel represents the BR-DCB bias ($\frac{\Delta d_{ru,2*} - \Delta d_{ru,1*}}{\mu_{2*} - \mu_{1*}}$) in SD ionospheric delays. We can see that in this case the BR-DCB can affect 'biased' SD ionospheric delays because their trends are consistent. This is, however, not unexpected, given their interpretation (see table 2).

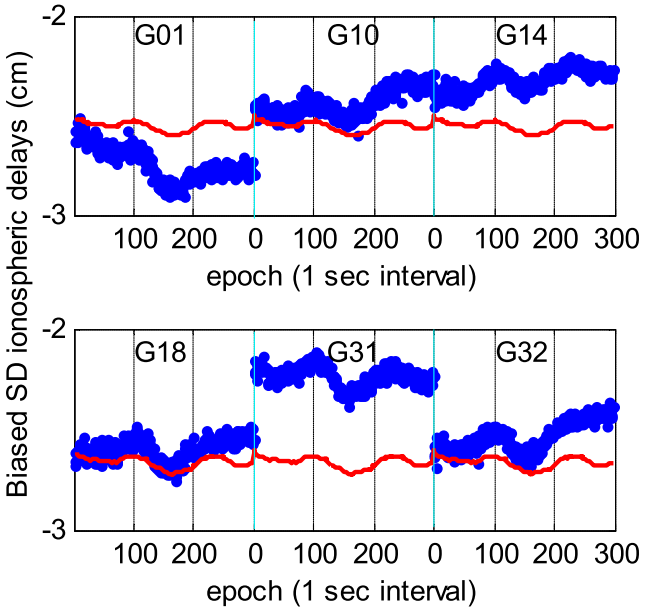

Figure 3. Biased ionospheric delays and BR-DCB change trend at the MC02-MC03 baseline over five minutes.

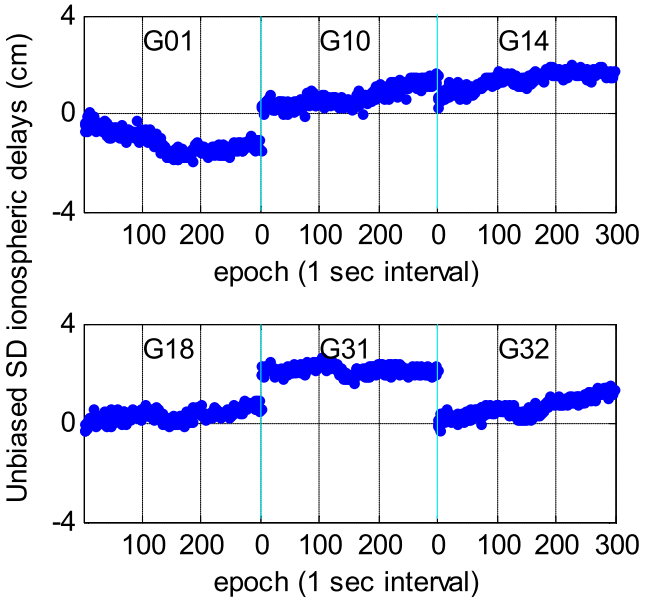

Figure 4. Ionospheric delay with BR-DCB eliminated at the MC02-MC03 baseline in five minutes.

In order to obtain high precision SD ionospheric delays, it is necessary to eliminate the effect of BR-DCB through an empirical ionosphere-weighted model. In figure 4, which is analogous to figure 3, expect that BR-DCB is removed from 'biased' ionospheric delays. In accordance with our expectations, these time series do not exhibit a consistency tendency. In this case, we can calculate the STD of the SD ionospheric delays as the variance of the observed values.

Based on the data in the network, a large number of results were obtained, including the accuracy of SD ionospheric delays at different time periods at different baselines and of different satellites. Considering the fact that a large set of results are available, we do not attempt to cover all of them, rather, without loss of generality and for the sake of clarity,

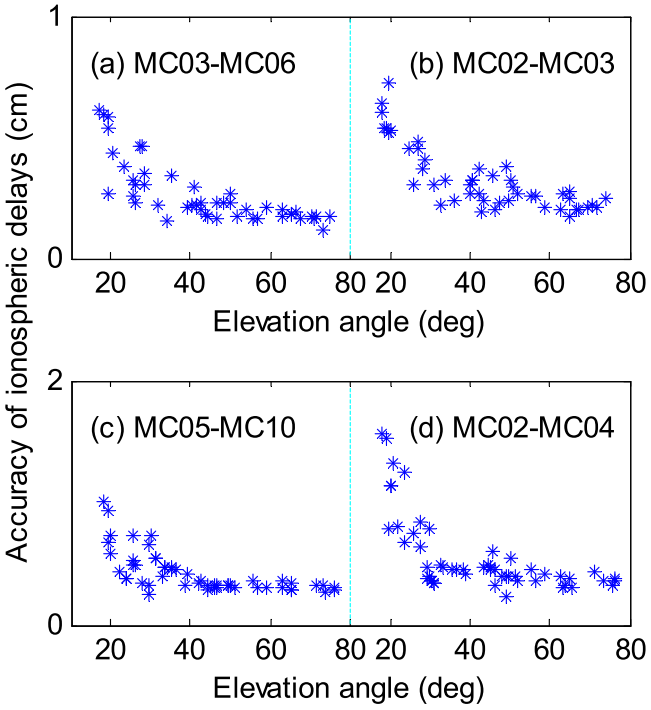

Figure 5. The relationship between the accuracy and elevation angle for four baselines ((a) MC03-MC06 with 11.06 km; (b) MC02-MC03 with 28.50 km; (c) MC05-MC10 with 35.80 km; (d) MC02-MC04 with 55.78 km).

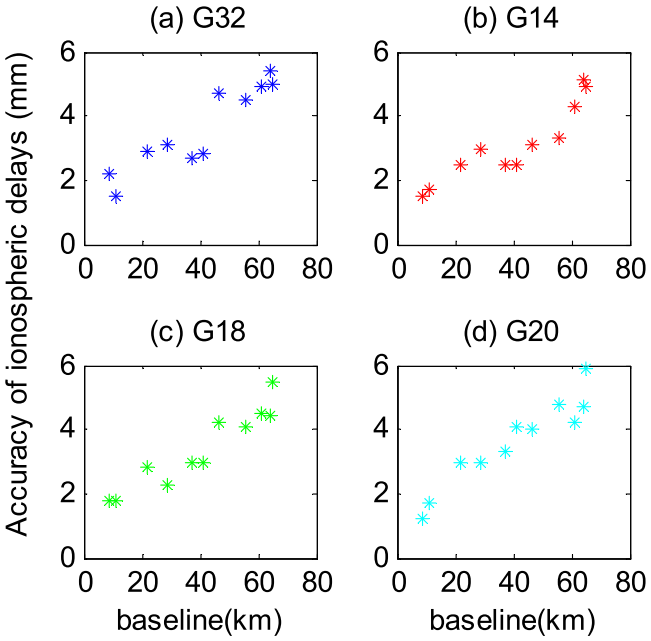

Figure 6. Relationship between accuracy and the baseline length of four satellites ((a) G32; (b) G14; (c) G18; (d) G20).

we only present the results for several receivers on September 5, 2018.

Let us focus first on figure 5, consisting of four panels, with each showing that the accuracy of ionospheric delays varies with elevation, using the same observation period. It is worth mentioning that four of the baselines involved here are of different lengths, from 10 kilometers to more than 50 kilometers. Two findings emerge here. First, there is a correlation between

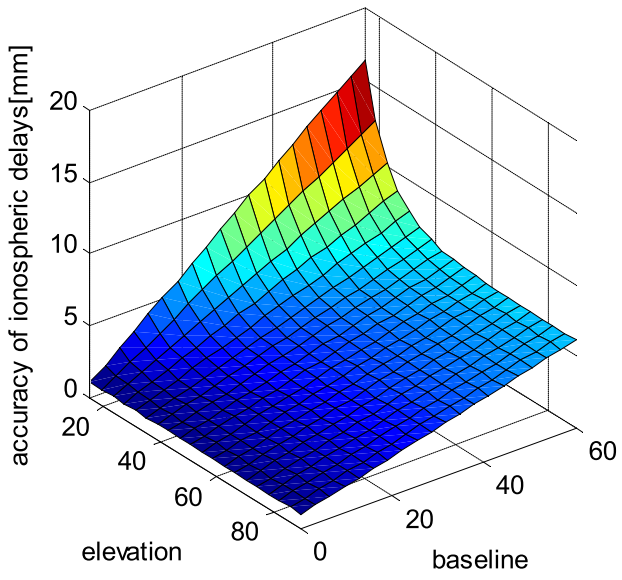

Figure 7. The relationship between the accuracy of ionospheric delays and the length of baseline and elevation obtained by matching.

ionospheric delay precision and elevation angle, as evidenced by the fact that the accuracy improves with the increase of elevation. Second, the accuracy decreases as the baseline length increases, with the length of the baseline increasing from (a)–(d).

Since the elevation of satellites observed by receivers at both ends of the same baseline are different, the relationship between baseline length and the accuracy of ionospheric delay was analyzed for different satellites over the same observation period. Satellites with low elevation are usually susceptible to frequent cycle slips as well as significant tropospheric delays, and are thus not involved in our analysis.

Figure 6 is analogous to figure 5, except that the horizontal axis now refers to the baseline length. It is worth mentioning that the four satellites examined here are divisible into two pairs, with each pair being located in high- (G32 and G24) and middle-elevations (G18 and G20), respectively. Similar to the second conclusion obtained when we analyzed the relationship between elevation and accuracy. From figure 6 one can see that it is feasible to establish a linear function according to the length of the baseline.

Notably, since ionospheric variance is related to the elevation and baseline length, we construct the empirical model as follows:

$$\hat{\sigma}_I = L_{\text{base}}(e_1 + e_2 \exp(^{-E^{m*}}/_{E_0})) + e_3 \qquad (10)$$

which is analogous to (4), except that L_{base} represents the baseline length in kilometers and e_3 is a model coefficient added.

Based on equation (10), the model coefficients of the ionospheric weighting function are obtained by the least-squares fitting. In this case, the ionospheric model coefficients e_1, e_2, E_0, e_3 are given as 0.0000846, 0.00096, 8.745 and 0.001045, respectively, and the fitting surface is shown in figure 7. In figure 7, we can clearly see the functional relationship among ionospheric precision, baseline length and elevation. The performance of this function is unknown and will be analyzed in detail.

Medium baseline RTK. Based on three baselines of different lengths above, four strategies are designed to show the impact of the ionosphere-weighted model calculated. All three baselines are taken from the NGS CORS network, and the details are presented in table 7. The strategies designed are as follows.

1. The ionosphere-float model of empirical observation weight is adopted, with 0.3 m for the code and 3 mm for the phase.
2. The ionosphere-float model with observation weighted by VCE result.
3. The ionosphere-weighted model used empirical observation weights, which is the same as strategy 1 and the empirical ionospheric weight used is 0.96 mm/km.
4. The ionosphere-weighted model with observations weighted by the VCE result and equation (10) is used as the ionospheric weighted function.

In the experiment, the Kalman filter is used for parameter estimation. The ionospheric and clock parameters are modeled as time-varying parameters. For the detailed analysis, we select an observation span of 3 h with an interval of 30 s (360 epochs) as an example and take the average of all the results as the final result.

The first figure of merit considered here is the time to first fix (TTFF), that is the time required before the first fixed solution is available. We reinitialize the filter after fixed ambiguity and the whole procedure is repeated again to obtain the average of the TTFF. Table 8 shows this measure for four strategies and for three baselines. The conclusions drawn from table 8 are as follows.

1. We focus first on the contrast strategies 1 and 2 with strategies 3 and 4, depicting the performance between the ionosphere-weighted and ionosphere-float models. We learn that, the ionosphere-weighted model, compared to ionosphere-float models, performs well for medium baseline lengths. In addition, it should be noted that the strategies 1 and 2 are intended to illustrate the importance of reasonable stochastic models for parameter estimation, and there is no doubt that strategy 2 performs better than strategy 1.
2. Attention is then paid to the contrast between strategies 3 and 4, which is the focus of our research. As we can see from NCSA-NCLE, which has a baseline less than 30 kilometers, both weighted models perform well. With an increasing distance between receivers, precise weighting performs significantly better than empirical weighting as shown in the reduced TTFF. The TTFF is reduced by a factor of approximately two for two baselines (NCWC-NCRE, NCSA-NCTR). We attribute this superior performance to the fact that the ionosphere-weighted model is highly likely to work well with a reasonable weight of ionospheric delays.

Table 7. Details of the three baselines used in the experiment.

Baseline	Receiver type	Length (km)	Location	Observation period	Sampling interval
NCSA-NCLE	Trimble NetR9	21.614	35 °N, 80 °W	2018, day 210-220	30 s
NCWC-NCRE		46.610			
NCSA-NCTR		63.701			

Table 8. TTFF needed for three baselines using different strategies.

	#epochs needed (The sampling interval is 30 s)			
Baseline	Strategy 1	Strategy 2	Strategy 3	Strategy 4
NCSA-NCLE	36	31	1	1
NCWC-NCRE	44	37	2	1
NCSA-NCTR	56	46	6	2

It is worth noting that, along with the reasonable weight of ionospheric observations, the ionospheric accuracy is also very important. The value of the observation is set as zero in this study, which limits model performance. We firmly believe that more accurate ionospheric information, combined with the precise weight distribution here, would be ideal for medium baselines with TTFF.

Now that the TTFF performance has been analyzed, it is natural to turn our attentions to analysis of the accuracy of the positioning results. Different from the ambiguity resolution analysis, the filters are not reset after ambiguity is fixed. Figure 8 shows three baselines calculated by different strategies. The coordinate correction values of the north, east and up are given. Each baseline is analyzed according to the above strategies 1, 2, 3, 4. It is worth noting that the truth coordinate values adopted in the experiment are derived from the real coordinates provided by NGS.

As expected, the ionosphere-weighted model significantly improves the positioning accuracy. First focusing on (a) NCSA-NCLE, the shortest baseline, the ionosphere-float model does not achieve the same effect as the ionosphere-weighted model until it has dozens of epochs. The performance of the two ionosphere-weighted models is also roughly the same because of the fixed ambiguities, which can be achieved without a long baseline. Then, we turn our attention to the other two baselines, both of which are over 40 kilometers. The time for the ionosphere-float model to converge becomes longer, because the ambiguity fixed is harmed by the residual ionospheric delays. Note that, even with the empirical ionosphere-weighted model, the ambiguities can hardly be resolved since the weight of the ionospheric observables used is not realistic.

Figure 9 shows the RMS results of the three baseline strategies, which correspond to figure 8. The graph shows the improvement when going from the ionosphere-float model with dm-level precision, to the ionosphere-weighed model with mm to cm-level precision, as well as the improvement which a reasonably weighting function brings. In this context, note that the ionosphere-weighted model, with the weighting model we raise, can achieve mm-level precision while the empirical one can only be mm-cm for north, east and up.

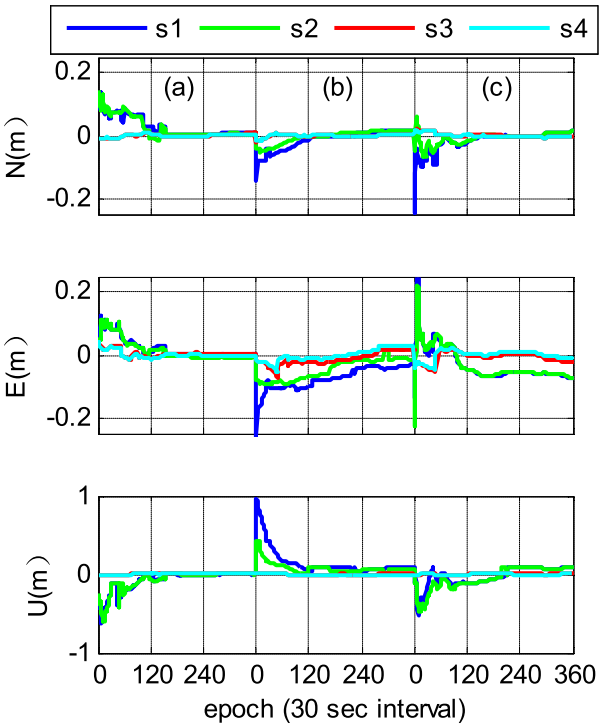

Figure 8. Baseline comparison of three baselines using different strategies. The left-hand column is (a) NCSA-NCLE, the middle column is (b) NCWC-NCRE, and the right-hand column is (c) NCSA-NCTR. The errors of north, east and up are given in the top, middle, and bottom rows, respectively. s1, s2, s3 and s4 in the figure represents the four different data processing strategies.

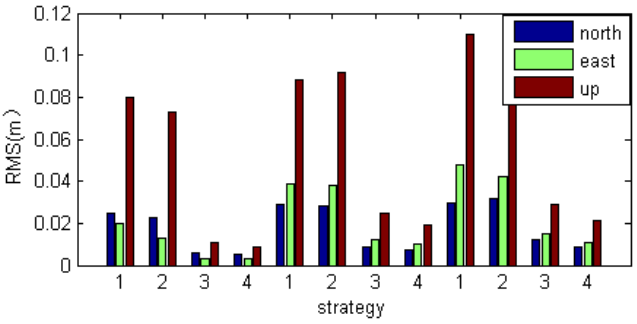

Figure 9. RMS of north, east and up obtained by the four strategies. The left-hand column is NCSA-NCLE, the middle column is NCWC-NCRE, and the right-hand column is NCSA-NCTR. The RMS results of each group of baselines are calculated according to the four strategies, which are represented by 1, 2, 3, 4 in figure.

Conclusions

The core contribution of this work is to construct reasonable stochastic model for the between-receiver SD ionospheric delays, used as pseudo observables in the ionosphere-weighted

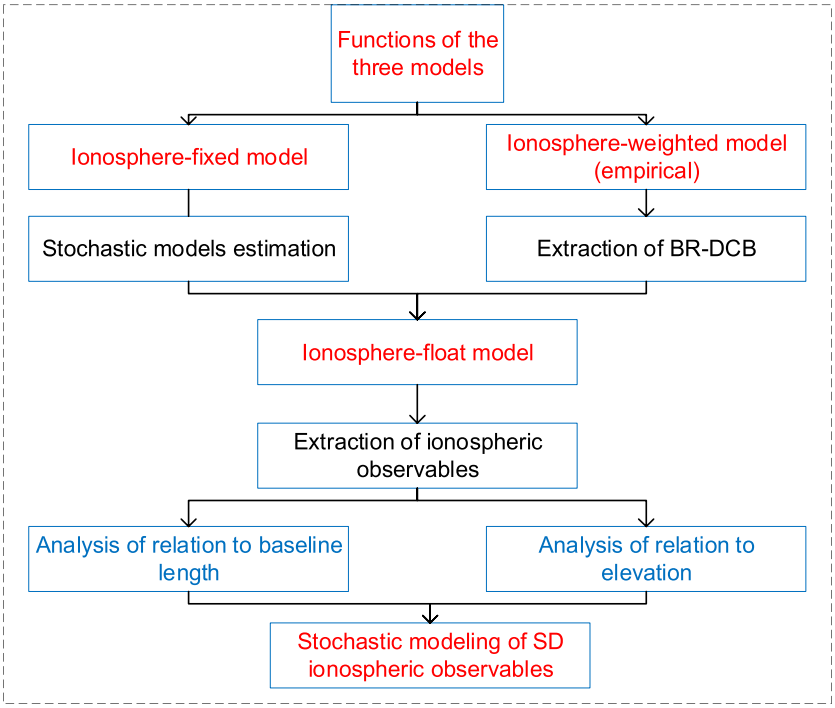

Figure 10. Functional schematic of the three models.

model, so as to raise the success rate of integer ambiguity resolution and further the positioning accuracy.

To achieve our goal, three models are used, including the ionosphere-fixed, -weighted and -float models; different models play different roles in the study, as suggested by figure 10. The ionospheric variance as a function of elevation as well as the length of the baselines is established. In addition, this work has strong practicability and reliability, and can effectively increase the inter-station distance of RTK positioning technology. However, this model is limited by time and space, so it is necessary to make corresponding modeling for specific areas.

We assessed the performance of the ionosphere-weighted model based on a set of GPS data from the National Geodetic Survey (NGS) CORS network. In our analysis, the time to first fix (TTFF) was investigated, and the positioning performance was evaluated by comparing the positions estimated to their ground truths. The results obtained thus warrant two conclusions.

First, in contrast to the ionosphere-float model, the ionosphere-weighted model is capable of reducing the time required to fix ambiguity to a large extent. For a medium baseline, the ionosphere-weighted model usually requires only a few minutes to firstly resolve the ambiguities while the ionosphere-float model takes much longer time.

Second, the ionosphere-weighted model, with observations and ionospheric delays weighted reasonably, can provide reliable ambiguity resolution in one minute even in the absence of any external ionospheric information. Use of the proper GNSS stochastic model as derived from the VCE method, along with the realistic ionospheric weighting strategy can ensure optimal RTK positioning performance in case of medium baselines.

Acknowledgments

Many thanks are due to the Curtin University and NGS for providing GNSS data. This work was funded by the National Natural Science Foundation of China (Grant Nos. 41604031, 41774042, 41621091). The second author is supported by the CAS Pioneer Hundred Talents Program. The third author acknowledges LU JIAXI International team program supported by the K C Wong Education Foundation and CAS.

ORCID iDs

Xiaolong Mi https://orcid.org/0000-0003-2950-3472

References

Amiri-Simkooei A 2007 Least-squares variance component estimation: theory and GPS applications *PhD Thesis* Delft University of Technology

Amiri-Simkooei A and Jazaeri S 2012 Weighted total least squares formulated by standard least squares theory *J. Geodet. Sci.* **2** 113–24

Amiri-Simkooei A R 2013 Application of least squares variance component estimation to errors-in-variables models *J. Geod.* **87** 935–44

Ananga N, Coleman R and Rizos C 1994 Variance-covariance estimation of GPS networks *Bull. Géod.* **68** 77–87

Böhm J, Heinkelmann R and Schuh H 2007 Short note: a global model of pressure and temperature for geodetic applications *J. Geod.* **81** 679–83

Crocetto N, Gatti M and Russo P 2000 Simplified formulae for the BIQUE estimation of variance components in disjunctive observation groups *J. Geod.* **74** 447–57

Euler H J 2004 Improvement of positioning performance using standardized network RTK messages *Proc. of ION NTM-2004 (San Diego, CA)* pp 453–61

Goad C C and Goodman L 1974 A modified hopfield tropospheric refraction correction model *American Geophysical Union Annual Fall Meeting (San Francisco, CA)* p 28

Grejner-Brzezinska D A, Wielgosz P, Kashani I, Smith D A, Spencer P S, Robertson D S and Mader G L 2004 An analysis of the effects of different network-based ionosphere estimation models on rover positioning accuracy *J. Glob. Position. Syst.* **3** 115–31

Grodecki J 2001 Generalized maximum-likelihood estimation of variance–covariance components with non-informative prior *J. Geod.* **75** 157–63

Julien O, Alves P, Cannon M E and Lachapelle G 2004 Improved triplefrequency GPS/Galileo carrier phase ambiguity resolution using a stochastic ionosphere modeling *Proc. IONNTM-2004* (San Diego, CA: Institute of Navigation) pp 441–52

Li B, Feng Y and Shen Y 2010 Three carrier ambiguity resolution: distance-independent performance demonstrated using semi-generated triple frequency GPS signals *GPS Solut.* **14** 177–84

Li B, Shen Y and Xu P 2008 Assessment of stochastic models for GPS measurements with different types of receivers *Chin. Sci. Bull.* **53** 3219–25

Liu G C 2001 Ionosphere weighted global positioning system carrier phase ambiguity resolution *PhD Thesis* University of Calgary

Liu X, Tiberius C and de Jong K 2004 Modelling of differential single difference receiver clock bias for precise positioning *GPS Solut.* **7** 209–21

Odijk D 2000a Weighting ionospheric corrections to improve fast GPS positioning over medium distances *Proc. ION GPS 2000 (Alexandria, Egypt)* pp 1113–23

Odijk D 2000b Stochastic modelling of the ionosphere for fast GPS ambiguity resolution *Proc. Geodesy Beyond 2000—the Challenges of the First Decade* (Birmingham: IAG General Assembly) vol 121 pp 387–92

Odijk D 2000c Improving ambiguity resolution by applying ionosphere corrections from a permanent GPS array *Earth Planets Space* **52** 675–80

Odijk D 2002 Fast precise GPS positioning in the presence of ionospheric delays *PhD Thesis* Delft University of Technology

Odolinski R, Teunissen P J and Odijk D 2013 Quality analysis of a combined COMPASS/BeiDou-2 and GPS RTK positioning model *Int. Global Navigation Satellite Systems Society IGNSS Symp. (Golden Coast, Australia, 16–18 July 2013)*

Odolinski R, Teunissen P J and Odijk D 2015a Combined BDS, Galileo, QZSS and GPS single-frequency RTK *GPS Solut.* **19** 151–63

Odolinski R, Teunissen P J G and Odijk D 2015b Combined GPS + BDS for short to long baseline RTK positioning *Meas. Sci. Technol.* **26** 045801

Saastamoinen J 1972 Contributions to the theory of atmospheric refraction *Bull. Geod.* **105** 279–98

Schaffrin B and Bock Y 1988 A unified scheme for processing GPS dual-band phase observations *Bull. Géod.* **62** 142–60

Teunissen P J 1999 An optimality property of the integer least-squares estimator *J. Geod.* **73** 587–93

Teunissen P J G 1995 The least-squares ambiguity decorrelation adjustment: a method for fast GPS integer ambiguity estimation *J. Geod.* **70** 65–82

Teunissen P J G 1997 The geometry-free GPS ambiguity search space with a weighted ionosphere *J. Geod.* **71** 370–83

Teunissen P J G 1998 The ionosphere-weighted GPS baseline precision in canonical form *J. Geod.* **72** 107–11

Teunissen P J G 2018 Distributional theory for the DIA method *J. Geod.* **92** 59–80

Teunissen P J G and Amiri-Simkooei A R 2008 Least-squares variance component estimation *J. Geod.* **82** 65–82

Teunissen P J, Odijk D and Zhang B 2010 PPP-RTK: results of CORS network-based PPP with integer ambiguity resolution *J. Aeronaut. Astronaut. Aviat. Ser* A **42** 223–30

Tiberius C and Kenselaar F 2003 Variance component estimation and precise GPS positioning: case study *ASCE J. Surv. Mapp. Div.* **129** 11–8

Tiberius C C J M and Kenselaar F 2000 Estimation of the stochastic model for GPS code and phase observables *Surv. Rev.* **35** 441–54

Wang J, Satirapod C and Rizos C 2002 Stochastic assessment of GPS carrier phase measurements for precise static relative positioning *J. Geod.* **76** 95–104

Wang N, Yuan Y, Li Z and Huo X 2016 Improvement of Klobuchar model for GNSS single-frequency ionospheric delay corrections *Adv. Space Res.* **57** 1555–69

Wanninger L 2002 Virtual reference stations for centimeter-level kinematic positioning *Proc. ION GPS 2002 (Portland, Oregon)* pp 1400–7

Wielgosz P 2011 Quality assessment of GPS rapid static positioning with weighted ionospheric parameters in generalized least squares *GPS Solut.* **15** 89–99

Wielgosz P, Kashani I and Grejner-Brzezinska D 2005 Analysis of long-range network RTK during a severe ionospheric storm *J. Geod.* **79** 524–31

Xu P, Shen Y, Fukuda Y and Liu Y 2006 Variance component estimation in linear inverse ill-posed models *J. Geod.* **80** 69–81

Zhang B and Teunissen P J G 2015 Characterization of multi-GNSS between-receiver differential code biases using zero and short baselines *Sci. Bull.* **60** 1840–9

Zhang B and Teunissen P J G 2016 Zero-baseline analysis of GPS/BeiDou/Galileo between-receiver differential code biases (BR-DCBs): time-wise retrieval and preliminary characterization navigation *J. Inst. Navig.* **63** 181–91

Zhang Z, Li B and Shen Y 2018 Efficient approximation for a fully populated variance-covariance matrix in RTK positioning *J. Surv. Eng.* **144** 04018005

Zhou P and Wang J 2013 Stochastic ionosphere models for precise GNSS positioning: sensitivity analysis *J. Glob. Position. Syst.* **12** 53–60